EREM 79/1

Journal of Environmental Research,
Engineering and Management
Vol. 79 / No. 1 / 2023
pp. 133–147
DOI 10.5755/j01.erem.79.1.33057

Use of Hydro-chemical Tools to Improve Definitions of the North-Western Sahara Aquifer System, Case of Ouargla Groundwater, Algeria

Received 2022/12 Accepted after revision 2023/03

https://doi.org/10.5755/j01.erem.79.1.33057

Use of Hydro-chemical Tools to Improve Definitions of the North-Western Sahara Aquifer System, Case of Ouargla Groundwater, Algeria

Feyrouz Hafid[1,*], Aziez Zeddouri[1], Hichem Zerrouki[2], Badreddine Saadali[2], Lassaad Ghrieb[3], Asma Nour El Houda Sid[4]

[1]Underground Oil, Gas and Aquifer Reservoirs Laboratory, Department of Earth Sciences and Universe, University of Ouargla, Algeria

[2]Department of Geology, University of Oum-El-Bouaghi, Algeria

[3]Faculty of Natural Sciences, Life Sciences, Earth and the Universe, University of Guelma, Algeria

[4]Research Unit of Materials, Processes and Environment, Faculty of Technology, M'hamed Bougara University, Boumerdes, Algeria

***Corresponding author:** feyrouz.hafid@univ-oeb.dz

The North-Western Sahara Aquifer System (NWSAS) is a complex multi-layered aquifer system with extraordinary continental groundwater reserves. This largest aquifer in the world straddles three countries: Algeria, Libya, and Tunisia. It contains more than 50,000 billion cubic meters of water; of which 70% is in Algerian territory in the southeast of the country. This water is the result of accumulation over 1 million years. In the Wadi Mya basin (Algeria), this system is characterized by two overlaid aquifer systems: the complex terminal (CT), a shallow aquifer housed in the Senonian-Eocene and Mio-Pliocene formations, and the continental intercalary (CI), a deep aquifer hosted in the Albian, Aptian and Barremian formations. The main purpose of this study is to carry out a correlation between the geochemical composition of the water and the facies of the aquifer formation. The adopted approach will allow deciphering the hydro-chemical relationships between the different levels of the two aquifer systems in the Wadi Mya basin. To acquire the chemical composition of water, the study method goes through a targeted sampling and physicochemical analysis of water followed by a statistical analysis as well as correlation and geochemical modelling: the interpretation of specific diagrams (Piper), correlations between chemical elements in binary graphs, and principal component analysis (PCA). The performed geochemical modelling by examining the saturation index and chemical balance of water helps to better understand the origin of mineralization, elucidate the mixing of waters originating from different aquifers, as well as highlight the relationship between deep and shallow aquifers in the Wadi Mya Basin hydrodynamic conversion. The obtained results indicate that the overall mineralization occurring within the study area is dominated by sodium chloride and calcium chloride-sulfate facies. This can be explained by the dissolution of halite, gypsum, and anhydrite evaporitic rocks, intercalated in the aquifer matrix besides the effects of the extended stay of fossil waters with low recharging and cation exchange reactions resulting from water-rock interactions. The interference recorded between the geochemical signatures of the two aquifers favors the hypothesis of interconnection between aquifers through fractures.

Through the implementation of such academic research, this invaluable source of life will stay sustainable for future generations.

Keywords: aquifer, mineralization, Wadi Mya, continental intercalary, complex terminal, interconnection.

Introduction

The development of Algeria during the current century will have to be carried out in the south of the country (OSS, 2015). The human activities in this arid climate and desertic environment, have depended mainly on groundwater resources of the NWSAS (OSS, 2003). The largest irrigated crops have basically been dependent on the deep boreholes capturing the Complex Terminal aquifer (CT) and the Continental Intercalary (CI) (Hamed et al., 2014; Kallel et al., 2017; Hamad et al., 2018; Besser et al., 2019). This has clarified the knowledge on the hydrodynamic functioning of aquifers and their hydrogeological characteristics, as highlighted by previous study projects carried out by the United Nations (UNESCO, 1972). The present study aims to use the hydrogeochemical analysis to improve definitions of the NWSAS through a physicochemical-based approach, with a particular emphasis on the relationship between hydro-chemical characteristics of water and the lithological nature of aquifers in the region of the lower valley of Wadi Mya.

To achieve this objective, the study is carried out based on the physicochemical analysis conducted in 2019 by the Algerian water authority of the City Ouargla, in the boreholes capturing the Senonian and Mio-Pliocene water tables belonging to the hydrogeological system of the CT and deep boreholes of the Albian belonging to the hydrogeological system of the CI.

The problem of groundwater chemistry has been addressed by innumerable research worldwide (Belkesier et al., 2018; Benmarce et al., 2021; Bouselsal and Saibi, 2022; Brahmi et al., 2021; Hamad et al., 2022, 2022; Ncibi et al., 2021; Nekkoub et al., 2020).

General setting

The geology of the study area is established by a Precambrian basement formed of metamorphic and eruptive rocks, covered by sediments, thousands of meters thick with an age that extends from the Cambrian to the Quaternary. These formations build the Saharan platform. Following the deformations suffered by the entire Paleozoic sedimentary series during the Hercynian phase, it took on a pleated and sometimes peneplain appearance, thus forming a large asymmetrical sedimentary basin, where the Ouargla basin is located and more exactly in the depression of Wadi Mya.

This depression is part of the Lower Sahara, known for its considerable aquifer reserves and also hydrocarbons (SONATRACH 2007).

We observe that the sedimentary cover at the level of the depression is very thick in the North (6000 m) and becomes thinner and thinner going towards the South-West (400 m) (Aliev, 1972).

The top of the series is of Miocene age (0 to 400 m) surmounted by dunes and ergs of the Quaternary. The whole rests on Mesozoic formations with a thickness greater than 4000 m; the latter is in angular discordance with Paleozoic formations following Hercynian erosion (*Fig. 1*) (Cornet, 1964). The faults affecting the depression of Wadi Mya (Aliev, 1972; Fabre, 1976) are highlighted by seismic surveys. These faults intersect the series from the Cambrian to the Lower Senonian. They are oriented South-East-North-West and cross the region of Ouargla by the East; consequently, these faults are at the origin of a possible interconnection between the various superimposed aquifers (Edmunds et al., 2003; Guendouz et al., 2003). Locally, the geology is identified by a correlation between the lithostratigraphic logs of boreholes up to 4250 m deep, which makes it possible to establish a geological section (*Fig. 2*).

Fig. 1. *Situation and hypsometry of the studied area*

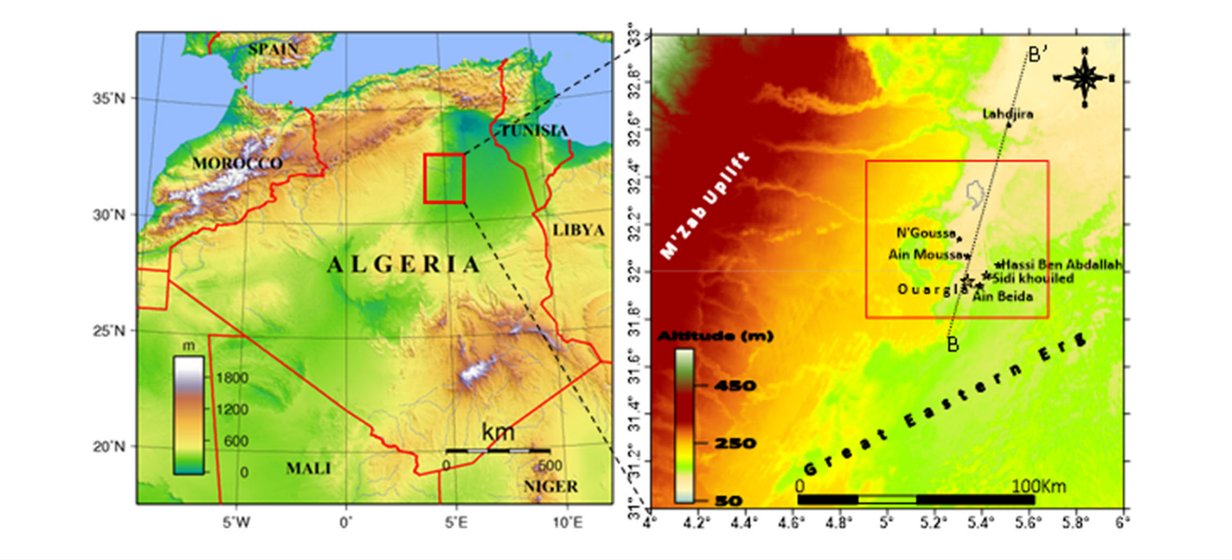

Fig. 2. *Lithostratigraphic section of the Ouargla basin*

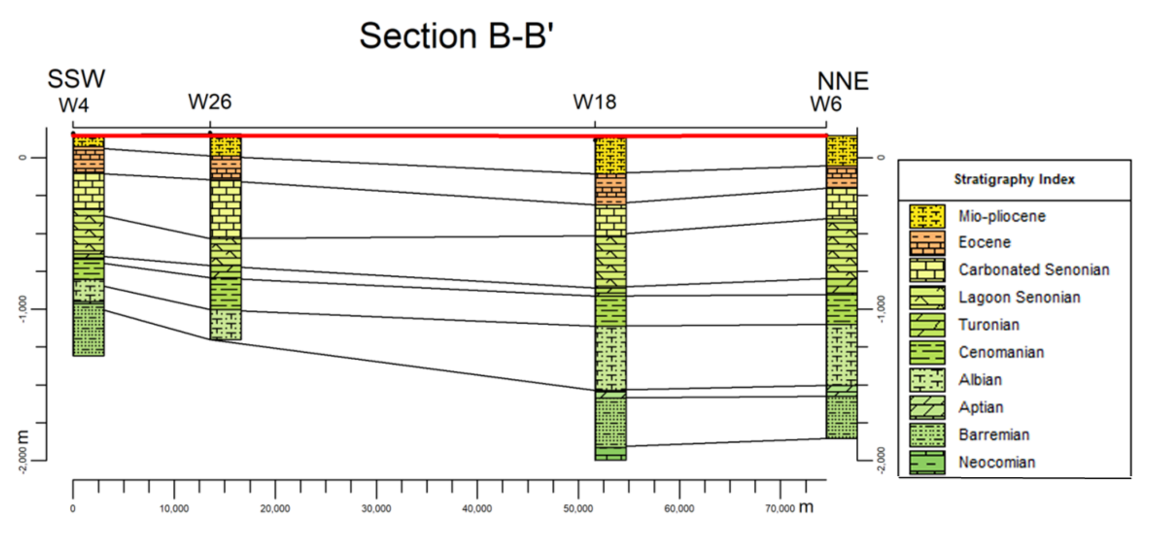

Hydrogeological context

The Wadi Mya basin contains important aquifers belonging to two main hydrogeological systems that overlap from top to bottom: the CT and the CI (ANRH, 2005; Cornet, 1964; UNESCO, 1972). The large water supply stored in these aquifers is ancient, inherited from past wet periods of the Holocene and Lower Pleistocene (Moulla et al., 2002).

The CT is hosted in the Senono-Eocene formations which are generally porous limestone with shell-like flints intercalated with marl and dolomite, at a depth of 120 to 200 m and with a thickness varying between 100 and 200 m, surmounted by sands of Mio-Pliocene age located at a depth of 20 to 100 m and its total thickness varies between 50 and 100 m, with a minimum of 20 m south of the city of Ouargla (Nadhira and Omar, 2019).

The CI water table is located at a greater depth of about 1100 to 1400 m, materialized by sandstone formations with clayey cement of Albian age and dolomite of the Aptian as well as Barremian sands, with a total average thickness of 640 m. Besides, the CI water quality is better than that of CT (Nezli, 2009) *Table 1*.

Table 1. *Lithostratigraphic and hydrogeological units in the Ouargla region. (OSS, 2003)*

ERA	SERIE	STAGE	LITHOLOGY	HYDROGEOLOGY	AQUIFER SYSTEM
Quaternary			Sands	Phreatic aquifer	Phreatic
			Clays, Evaporate	Bedrock	Impermeable
Cenozoic	Mio-Pliocene		Sands	Sandstone aquifer Continental Terminal	Complex terminal
			Gypsies clays		
		Pontian	Sand, Gravel, Sandstone	Sandstone aquifer Continental Terminal	
	Eocene		Laguna clay	Semi-permeable layer	
Mesozoic	Upper Cretaceous	Upper Senonian	Limestone	Calcareous aquifer Continental Terminal	
		Lower Senonian	Clay	Bedrock	Impermeable
		Turonian	Dolomite	Salt aquifer	
		Cenomanian	Clay, Marl	Bedrock	
	Lower Cretaceous	Albian	Sand, Sandstone	Albian Aquifer	Continental intercalary
		Aptian	Dolomite		
		Barremian	Sand		
		Neocomian	Clay, Anhydrite		
	Jurassic	Upper Jurassic	Limestone, Clay	Substratum	Impermeable

Methodology

A water sampling campaign by direct pumping from the wells was carried out in the study area during the month of February 2019 on a total of 48 deep boreholes, 21 capturing the CT aquifer and 27 boreholes drawing from the CI aquifer. The location of the sampled wells is shown in *Fig. 3*. Physical parameters including electrical conductivity (EC), total dissolved solids (TDS) and hydrogen potential (pH) were measured on site using a Hanna model multiparameter. Samples for major ion analyses were filtered (0.45 mm, paper filter), collected in 1 L capacity polyethylene bottles and analyzed within 72 hours. The chemical analyses were carried out at the Water Quality Control Laboratory of Algerian water company of Ouargla-Algeria (ADE). To test the reliability of the results, the ion balance set itself on an error coefficient of less than ± 5% (BRGM, 1971), which confirms a relatively good ionic balance.

Fig. 3. *Location map of sampled water wells*

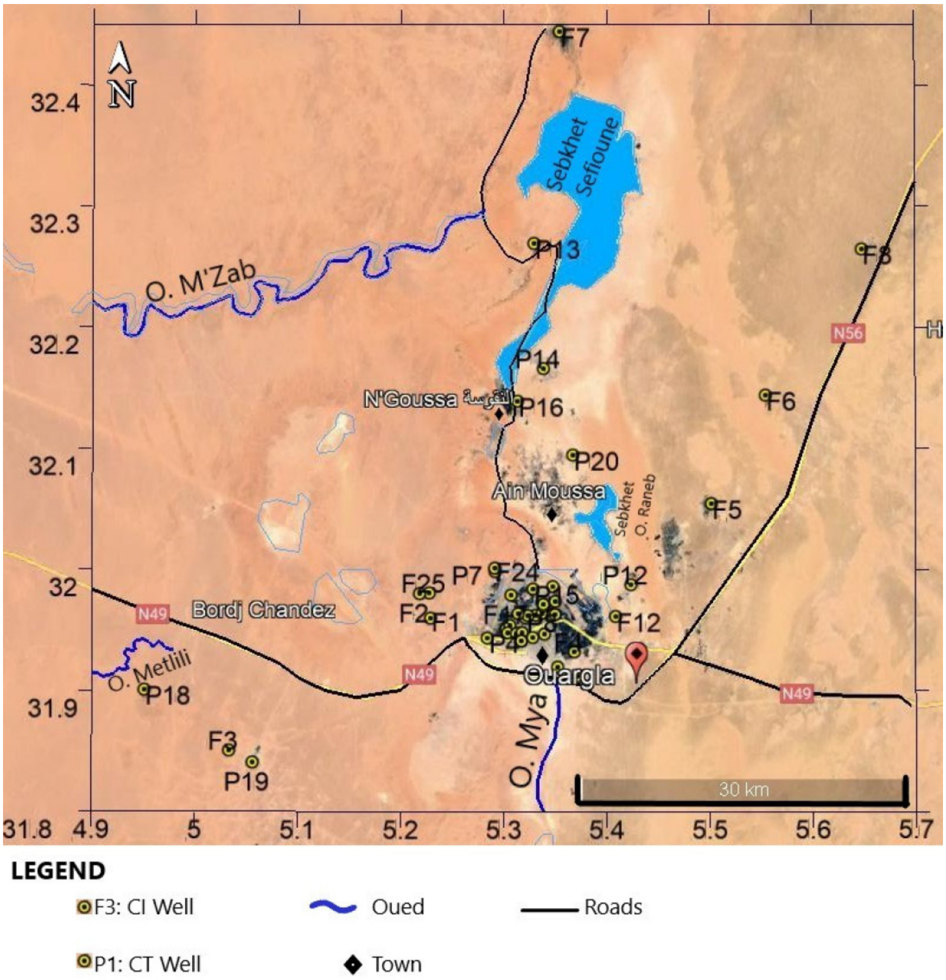

Table 2. *The physicochemical parameters of the 48 groundwater samples*

Variables	Units	Minimum	Maximum	Mean	Standard Deviation
pH	-	6.80	8.48	7.71	0.46
CE	µS/cm	1900.00	5430.00	2952.08	818.32
TDS	mg/L	1451.00	3574.00	1986.35	499.55
Ca^{2+}	meq/L	3.14	18.20	8.59	3.20
Mg^{2+}	meq/L	6.01	29.71	10.78	4.37
Na^{+}	meq/L	8.48	26.10	13.16	4.30
K^{+}	meq/L	0.15	1.82	0.58	0.38
HCO_3^{-}	meq/L	0.16	4.05	2.33	0.93
Cl^{-}	meq/L	8.60	30.60	16.03	5.96
SO_4^{2-}	meq/L	7.91	33.83	14.70	4.68

Results and Discussion

Chemical facies

Piper's triangular diagram (Piper, 1944) shows the effect of lithologic facies on the nature of the water and allows the estimation of the percentage of chemical elements. The diagram (*Fig. 4*) shows that the dominant anions in the water samples are chloride and sulfate while the dominant cations are sodium and calcium. Two types of water are present in the aquifer system: $Cl–SO_4–Ca$ and Cl-Na. Gypsum, halite, and other minor salts occur in many geologic units and are the major contributors to salinity. The major ions of these minerals and their saturation states are used to explore mineralization processes.

Statistical analysis

The statistical analysis of physicochemical parameters was performed using the statistical software XLstat, version 7.5.2, developed by Addinsoft. This method allows the determination of the relationships between the ionic constituents measured in CI and CT aquifers and the geological context (Esbensen, 2002). Groundwater properties are described by 9 variables (*Figs. 5a* and *5b*) from 21 samples collected in the CT and 27 samples in the CI, namely ions concentration (Ca^{2+}, Mg^{2+}, Na^{+}, K^{+}, Cl^{-}, SO_4^{-2}, HCO_3^{-}) measured in the laboratory as well as total mineralization (TDS), pH, and electrical conductivity (EC) measured *in-situ*.

For the CT aquifer, the main factorial plane (F1–F2) is found to be the most important with a total percentage of 78.19% of the total variance, which is relatively large and thus indicates a close dependence between variables. The F1 axis (58.64%) indicates that all variables are positively correlated except pH, which represents the natural mineralization of the aquifer water acquired by the elements (Ca^{2+}, Mg^{2+}, Na^{+}, K^{+}, Cl^{-}, HCO_3^{-} and SO_4^{2-}), as shown in *Fig. 5a*. The F2 axis (19.55%) shows an opposition of two groups: (i) the positive side of the axis (Mg^{2+}, SO_4^{2-}, HCO_3^{-}, TDS and pH) constituting the pole of sulphates and bicarbonates, and (ii) the negative side of the axis (CE, Na^{+}, Cl^{-}, Ca^{2+} and K^{+}) presenting the pole of halite and in perfect agreement with the measured conductivity (Dhaouadi et al., 2021).

For the CI aquifer, the main factorial plane is mostly F1–F2 with 82.47% of the total variance (*Fig. 5b*), which is important because the concentrations of ions are in appropriate proportion. Indeed, F1 axis holds 57. 31% of the variance with a positive pole constituted by (CE, Ca^{2+}, Mg^{2+}, TDS, Na^{+}, Cl^{-}, SO_4^{2-}) and another negative marked by (pH, K^{+}, HCO_3^{2-}), which represents the impact of the dissolution of evaporites on CI water chemistry. Meanwhile the F2 axis has 25.16% of variance with a positive pole regrouping all the elements except Cl^{-} which is at the negative pole.

Fig. 4. *Piper diagram of CT and CI groundwater samples*

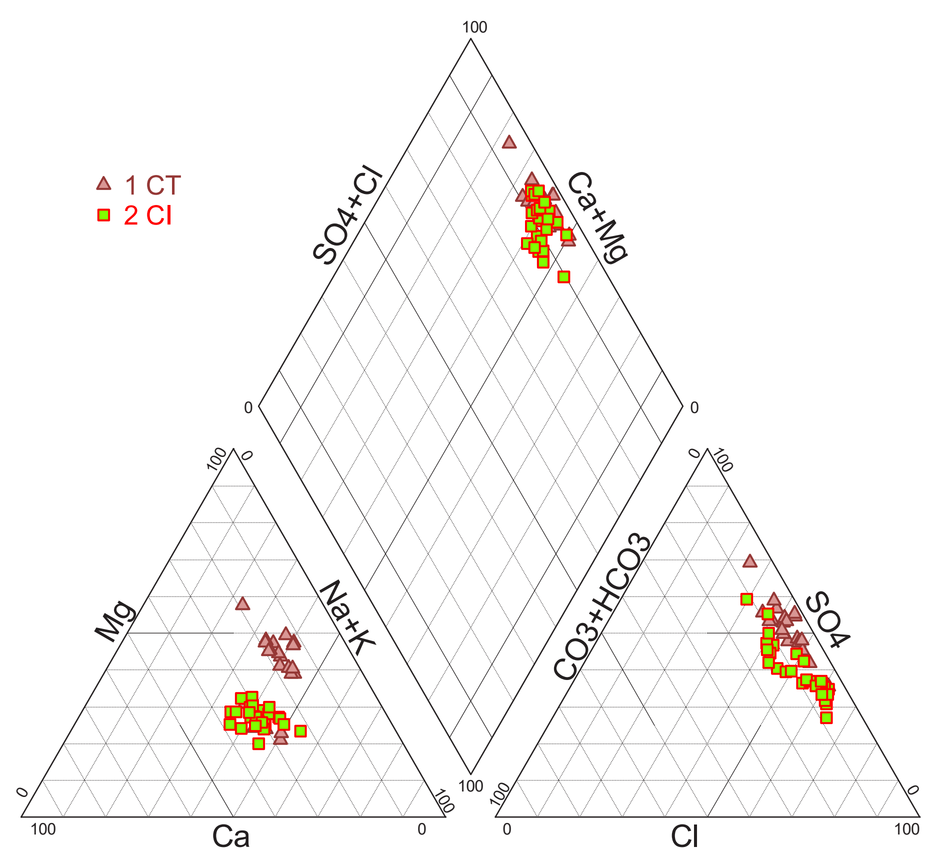

Fig. 5. *Principal component analysis (PCA); a) CT layer; b) CI layer*

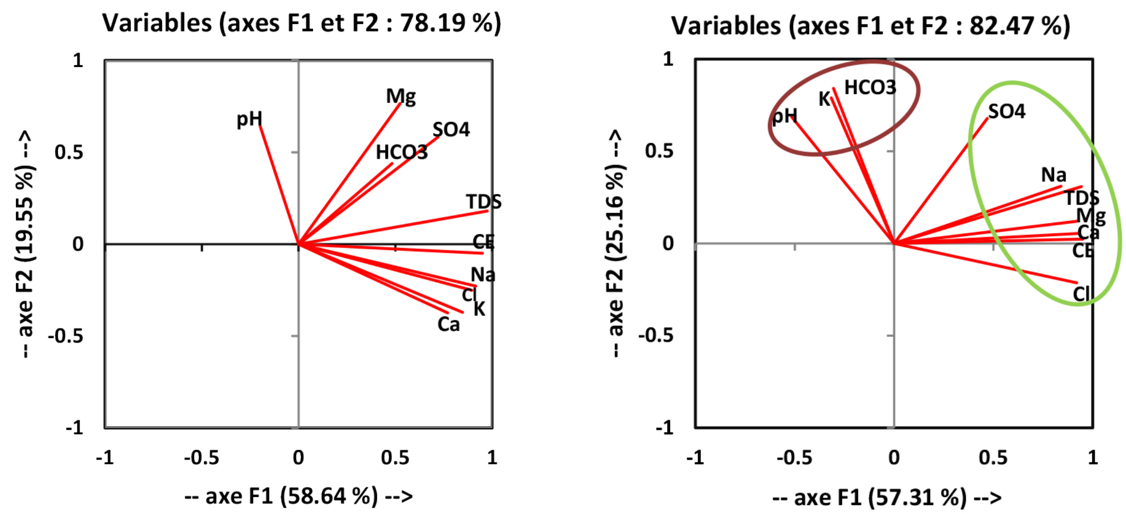

(a) *(b)*

Also, this axis is expressed by a strong positive charge on the pH, mainly associated with the precipitation of carbonates. The existence of remarkable positive correlations is also noted between (TDS, EC, Na^+, Ca^{2+}, Mg^{2+}, Cl^-, SO_4^{2-}) group and (K^+, pH, HCO_3^-) group, reflecting a direct proportionality between these elements, while the pH correlates negatively with CE, Ca^{2+} and Cl.

Origin of mineralization and correlation of ions

The origin of Na^+ and Cl^- ions is attributed to the dissolution of halite (NaCl) (Olivier, 2005), as confirmed by the group of points that are aligned along $Cl^-=f[Na^+]$ curve (*Fig. 6a*). These water samples are from both aquifers (CI and CT). This is confirmed by the positive correlation between chloride and sodium with a coefficient of determination (R^2) equal to 0.94 for the CT and 0.56 for the CI. The correlation in the binary diagram (*Fig. 6*) also shows that both aquifers present a set of points mostly below the slope line = 1; in this case, there is an enrichment in chlorine, which is more important for CI waters. This enrichment in chlorine is related to other sources apart from the dissolution of halite, and in counterpart, there is a loss in sodium, probably related to an interaction of waters with the reservoir rock. This loss will be compensated by Mg^{2+} and Ca^{2+} (Vengosh A, 2003; Kloppmann et al., 2011).

The obtained results convey the hypothesis that these waters have the same origin because of the contact between the two aquifer systems. However, this contact is not total; in fact, it occurs in some places with a discontinuous trend which can be directly associated directly to fractures or faults affecting the layer separating the two aquifers.

Fig. 6. *Binary diagram between chemical ions*

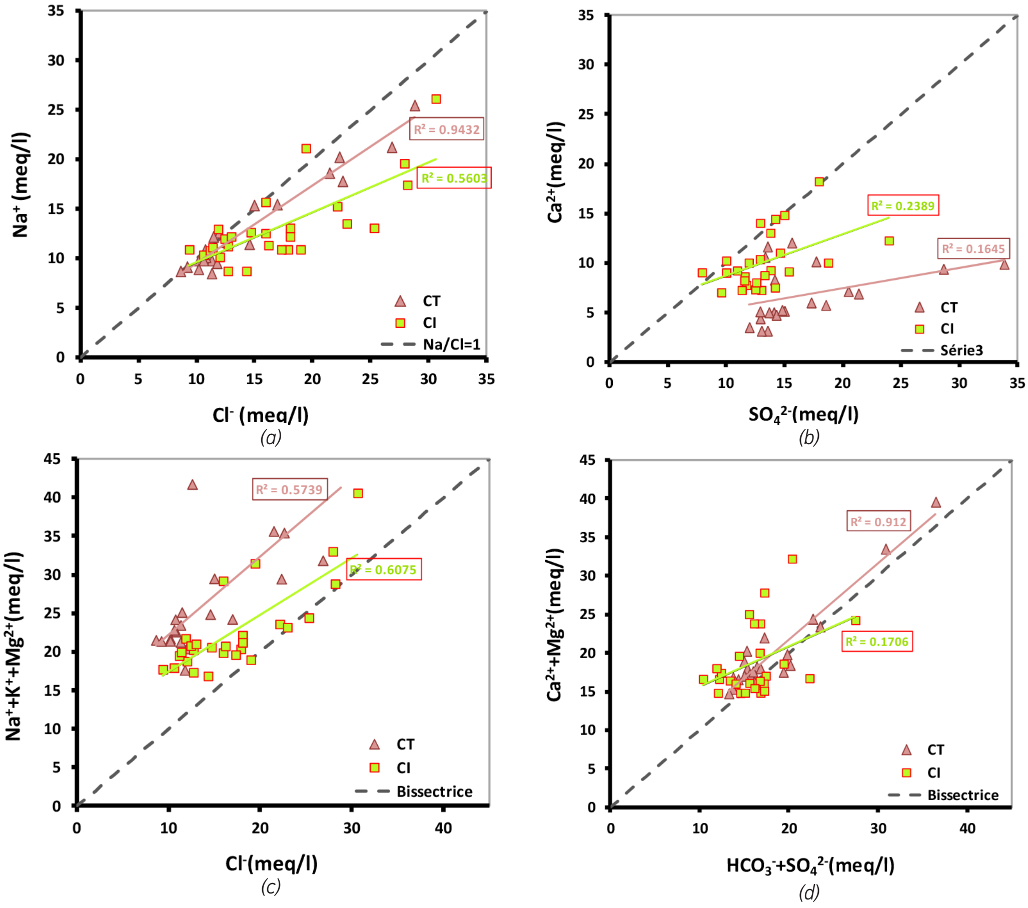

(a) *(b)* *(c)* *(d)*

The correlation in the binary diagram of calcium and sulfate ions $Ca^{2+}= f[SO_4^{2-}]$, as shown in *Fig. 6b*, shows that a good number of CI water table samples are on or near the slope = 1 line, implying that the origin of these waters is from the dissolution of gypsum. Besides, the rest of the CI waters are characterized by an enrichment in SO_4^{2-} because all the points are below the gypsum dissolution line, with a characteristic ratio rCa^{2+}/rSO_4^{2-} lower than 1 (*Fig. 6b*).

Further, it can be noted that sulfates are more dominant in the CT layer than in the IC layer. The calcium deficiency is attributed on the one hand to the precipitation of minerals in the form of calcite, dolomite, and aragonite (supersaturation of carbonates in the water) as confirmed by positive saturation indices, and on the other hand to the negative values of the base exchange index which characterizes part of the basin as defined by Schoeller (1962). The waters often exchange alkaline earth ions for alkaline ions, and it is the clays intercalated between the levels of the aquifer that release alkaline ions (Na^+ and K^+) and fix the alkaline earth ions (Ca^{2+} and Mg^{2+}). It is seen that the waters of the two aquifers can be differentiated in two clouds with more or less separate points, confirming unlike origins of these waters, except that five points still suggest the hypothesis of exchanges between the aquifer systems.

The variation of Na+, Mg2+ and K+ concentrations as a function of the Cl- anion concentration (*Fig. 6c*) reveals a positive linear correlation with a coefficient of determination close to 0.6 for both aquifers (CT and CI) and with a cloud of points lying above the dilution line of the salts. This confirms an enrichment in Na+, K+ and Mg2+ cations, and consequently an additional contribution arising from different origin. The interference in the cloud of points between the two aquifers (CT and CI) confirms the hydrodynamic exchanges of these waters.

Furthermore, from the curve illustrating the variation of $(Ca^{2+} + Mg^{2+})$ concentration vs. $(HCO_3^- + SO_4^{2-})$ concentration (*Fig. 6d*), it is observed that the points are distributed on and on either side of the slope line 1, highlighting the coexistence of two dissolution mechanisms.

This is due to the complexity of the aquifer system of the two sheets, since the first is dominated by carbonate essentially dolomitic, whereas the second mode of dissolution occurs by evaporation (gypsum and anhydrite).

The chloro-alkaline indices (CAI) can be positive or negative depending on the exchange of sodium and potassium in the rock with magnesium and calcium in the water and vice versa. It is obtained by the following relation (Schoeller H. 1962):

$$CAI = \frac{[rCl^- - r(Na^+ + K^+)]}{rCl^-} \tag{1}$$

Where three cases can be classified as follow: (i) $CAI < 0$: Ca^{2+} and Mg^{2+} ions present in the water are exchanged for K^+ and Na^+ ions in the surrounding formations. (ii) $CAI > 0$: Na^+ and K^+ ions from the water are replaced by Mg^{2+} and Ca^{2+} ions from the surrounding formations. (iii) $CAI = 0$: there is an equilibrium between the chemical compositions of the water and the surrounding formations.

Fig. 7 depicts the evolution of CAI. It is noted that all the studied samples show that two ion exchange mechanisms coexist in groundwater such as direct exchange and reverse exchange but with a dominance of a positive CAI.

Fig. 7. *Chloro-alkaline index*

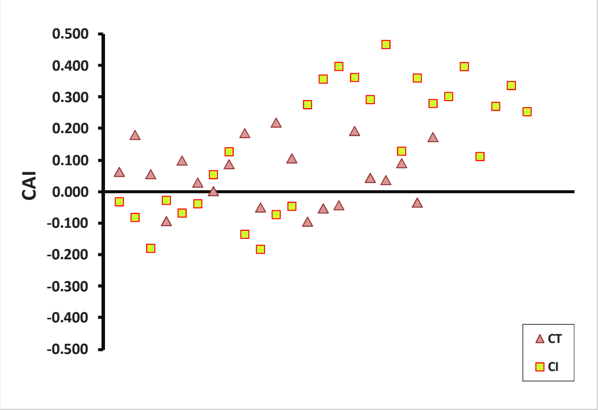

These exchanges are elucidated by the relationship $[(Ca^{2+}+Mg^{2+})-(HCO_3^-+SO_4^{2-})]$ as a function of $(Na^+ + K^+ - Cl^-)$ (Dassi, 2004; Garcia et al., 2001) and represented in *Fig. 8b*. This correlation highlights the reactions that can exist between clay minerals and water by subtracting ions from possible dissolutions of carbonate and evaporite minerals. In the absence of exchange, all representative sample points should be placed near the origin (McLean et al., 2000), which is the case for most of CT waters. However, for CI waters, the correlation manifests an inverse proportionality translated by a depletion in (Na^++K^+) accompanied by an increase in (Ca^{2+}+Mg^{2+}), and the phenomenon is also confirmed by CAI values. Indeed, this is the chemical signature of the carbonate and clay formations constituting the CI added to the long water-rock contact.

The observed ion exchange processes also contribute to the increase in the values of the ratio rNa^+/rCa^{2+} (*Fig. 8a*), which is always higher than 1 for both aquifers with some exceptions for the CI. In addition, the values of the ratio rNa^+/rMg^{2+} are higher than 1 for almost all the waters of the CI aquifer, indicating the dominance of the halite matrix over the carbonate matrix. Meanwhile, the excess of Na^+ besides the deficiency of Ca^{2+} to the benefit of SO_4^{2-} ions, leads to the appearance of sodium sulfate facies (Na-SO4).

From the above findings, it can be concluded that the waters of the two aquifers present a geochemical signature that is influenced by the evaporite matrix, notably halite, as well as by the long duration of the water-rock contact for CI waters with interferences. This confirms the communication between these two aquifer systems (Hamed et al., 2018).

In the diagram representing the weathering of dolomite and gypsum (*Fig. 9a*), it should be mentioned that the dissolution of (Mg^{2+}+Ca^{2+}) in groundwater is a major key to understanding the dolomite source rock under moderate TDS conditions.

If, however, the ratio of [(Mg^{2+})/(Ca^{2+}+Mg^{2+})] approaches 1, it is very likely that Ca^{2+} has been removed from the solution and this process is commonly referred to as dedolomitization. Hounslow (2018) suggests the following cases upon the value of [(Mg^{2+})/(Ca^{2+}+Mg^{2+})]: (i) = 0.5 reflects the dissolution of gypsum; < 0.5 for limestone-dolomite alteration; > 0.5 indicates the dissolution of dolomite alongside the precipitation of calcite.

From *Fig. 9b*, it is observed that in most CI waters samples, the values of the ratio are equal or lower than to 0.5, indicating the occurrence of two chemical processes within this reservoir including gypsum dissolution and/or limestone-dolomite alteration. Meanwhile, for most CT waters, this ratio is superior to 0.5, which means dissolution of dolomite and precipitation of calcite. The note in this diagram (*Fig. 9a*) reveals the appearance of two distinct clouds of points, at the bottom of the line [(Mg^{2+})/(Ca^{2+}+Mg^{2+})] = 0.5 representing the waters of the CT aquifer and at the top corresponding to the waters of the CI with a few points of CT waters. This implies an ascending supply

Fig. 8. *Correlation diagram: (a) Na^- vs. Ca^{2+}, (b) $[(Ca^{2+} + Mg^{2+})–(HCO_3^- + SO_4^{2-})]$ vs. $(Na^+ + K^+ – Cl^-)$*

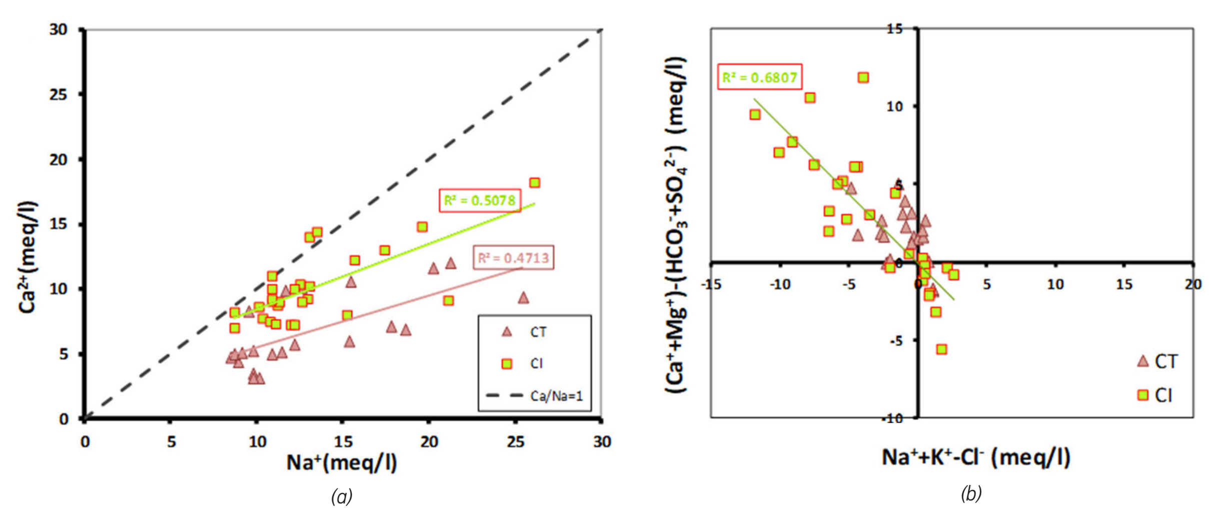

Fig. 9. *(a) Diagram for dolomite weathering type, (b) diagram for gypsum weathering type*

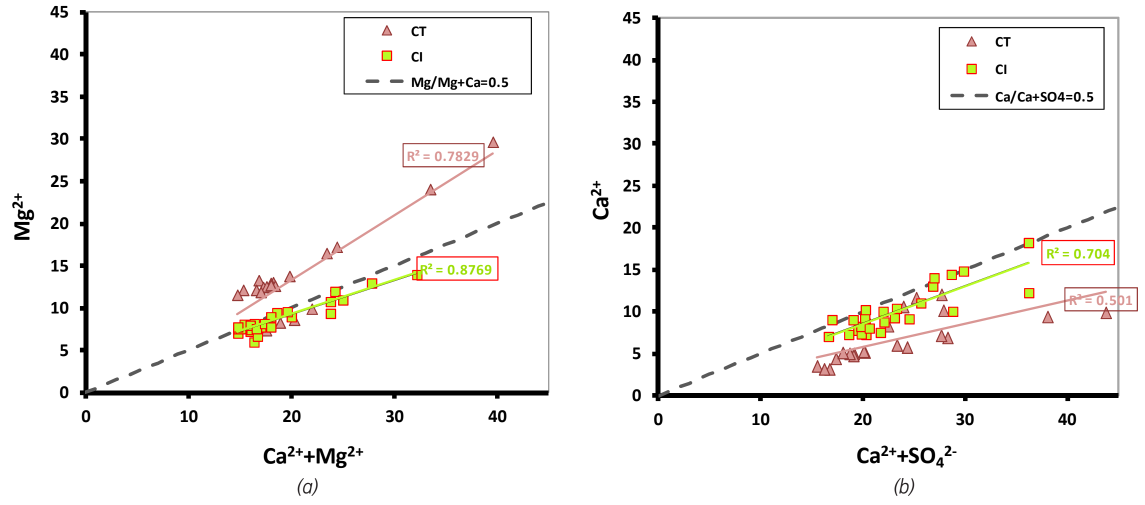

(a) *(b)*

of the CT aquifer by the waters of the CI, through local cracks and fractures.

Also, by applying the Hounslow equation, the gypsum type source rock can be deduced according to the categories of the [$(Ca^{2+})/(Ca^{2+}+SO_4^{2-})$] ratio: = 0.5 for gypsum dissolution; < 0.5 and pH < 5.5 for the oxidation of pyrite or ion exchange; < 0.5 and pH = neutral for the precipitation of calcite; > 0.5 for calcium sources other than carbonates and gypsum or silicates.

In *Fig. 9b*, two processes may occur, namely ion exchange or calcite precipitation. This rule applies to both aquifers (CI and CT) with some exceptions of gypsum dissolution for CI waters. However, the dominance of gypsum dissolution can be noted in both curves (*Fig. 8b*) and specifically for CI waters, and consequently the possible occurrence of water-anhydrous formation interactions of the Neocomian constituting the bedrock of the CI water table in the study area.

Geochemical modelling

The saturation index (SI) expresses the degree of chemical equilibrium between water and mineral in the aquifer matrix, and is considered as a measure of the dissolution and/or precipitation process for water-rock interaction (Drever, 1997). Using the geochemical program PHREEQC (Plummer et al., 1976) and the Aquachem software, the saturation index for anhydrite, aragonite, calcite, dolomite, gypsum, and halite has been calculated using equation (2), and the results are given in *Table 3*.

Table 3. *Saturation indexes of minerals in groundwater, with statistical summary using PHREEQC*

SI	Mean	Max	Min	SD
Aragonite	0.1475	0.77	-0.62	0.40291755
Calcite	0.29083333	0.91	-0.47	0.40142742
Dolomite	0.80916667	2.11	-0.87	0.88234657
Anhydrite	-1.05479167	-0.74	-1.44	0.16880039
Gypsum	-0.83520833	-0.52	-1.22	0.16895158
Halite	-5.46854167	-4.88	-5.86	0.25250228

The saturation Index (SI) of the selected mineral phase (degree of saturation, default value 0) is defined by the following equation:

$$SI = log\left(\frac{IAP}{KT}\right) \tag{2}$$

Where: IAP is the ion activity product for the given material and KT is the reaction constant at the given temperature. If $SI > 0$, the solution is supersaturated for the mineral phase. If $SI < 0$, the solution is below saturation of the specified mineral phase. If $SI = 0$, the solution is in equilibrium with the specified mineral phase.

The results for all the analyzed groundwater samples (*Table 2*) show that the water is always undersaturated in anhydrite, gypsum, and halite; meanwhile, it presents an oversaturation in aragonite, calcite, and dolomite with some exceptions of undersaturation. The saturation index of mineral species indicates that only carbonates tend to precipitate mainly as dolomite. This is because of their low equilibrium constants leading to rapid precipitation of these minerals in the water. However, the evaporated minerals are always undersaturated, due to their high equilibrium constant values, which allows the evaporated elements to coexist at high concentrations in water.

Fig. 10a and *10b*, illustrating the strong correlations between the saturation index of the waters for halite/gypsum as a function of (Na^++Cl^-)/(Ca^{2+}+SO_4^{2-}), support the hypothesis of the evaporites dissolution in the waters of the two aquifers (CT and CI). Thus, two distribution modes of the scatter plot in *Fig. 10b* can be highlighted: (i) individualizing the hydro-chemical signature of each type of aquifer, but with a slight saturation of the waters of the CI aquifer compared

Fig. 10. *Correlation of saturation indexes: a) halite vs. (Na^++Cl^-); b) gypsum vs. (Ca^{2+}+SO_4^{2-}); c) dolomite vs. (Ca^{2+}+Mg^{2+}+HCO_3^-); d) calcite vs. (Ca^{2+}+HCO_3^-)*

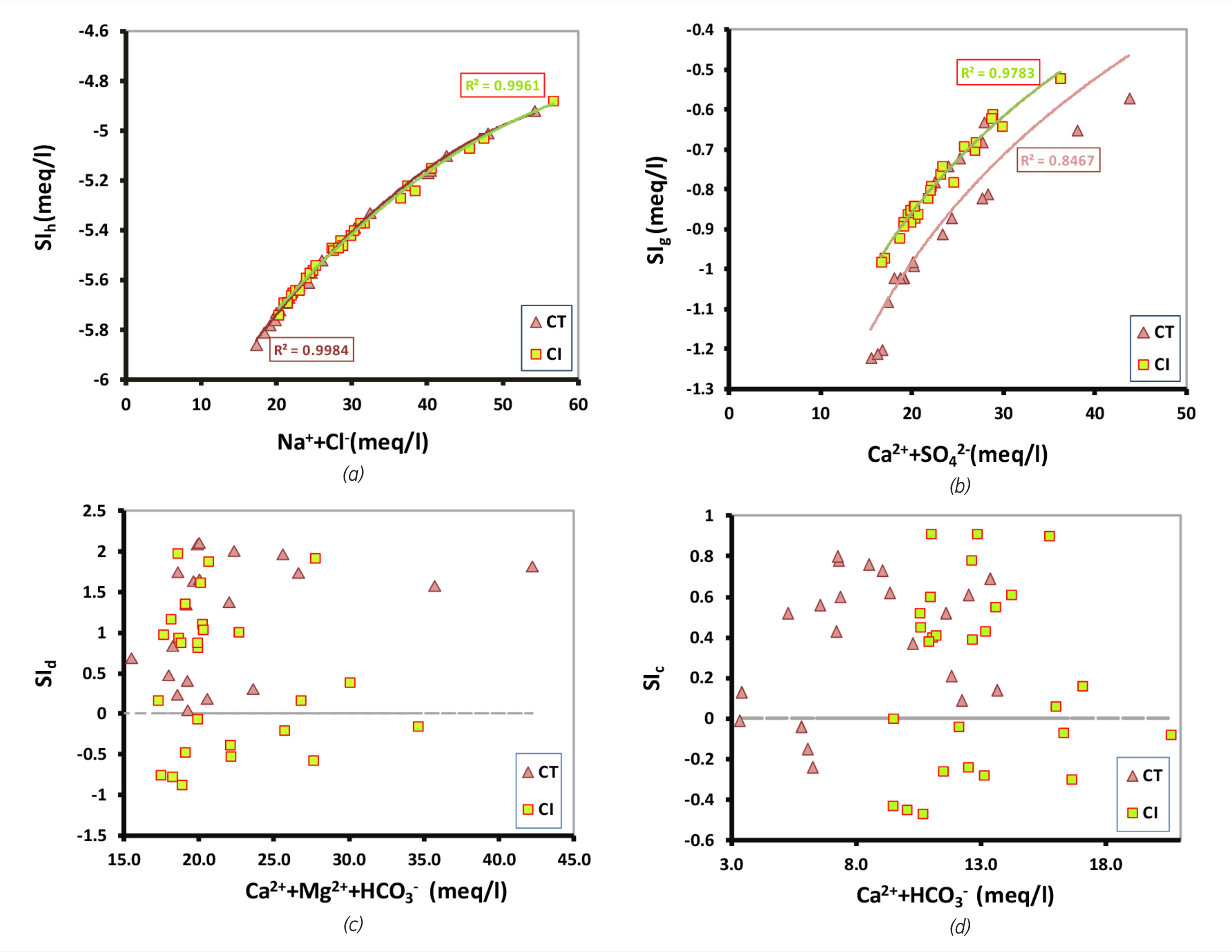

(a)

(b)

(c)

(d)

to that of the CT waters, given the long stay of these waters in the reservoir; (ii) some interference of the CT in the CI waters relative to the same origin, thereby explaining the existence of a probable interconnection between these aquifers.

Meanwhile, the absence of clear correlations between the saturation indices of calcite as a function of (Ca^{2+}+HCO_3^-) (*Fig. 10d*) and dolomite as a function of (Ca^{2+}+Mg^{2+}+HCO_3^-) (*Fig. 10c*) confirms the hypothesis of non-dissolution of these carbonate minerals, despite the few cases of undersaturation observed mainly for the CI waters.

Conclusion

This study showed that the waters of the aquifer system in Ouargla are composed of sodium chloride and calcium sulfate chloride facies. The principal component analysis proved the strong correlations between Na^+ and Cl^- for both aquifers, which is attributed to the dissolution of halite. Indeed, the evaporite matrix, and more particularly the halite, gives the water a dominant sodium chloride facies, with a coefficient of determination R^2 (Na^++Cl^-) = 0.94 for the CT waters and 0.56 for the CI waters. The coefficients of determination R^2 (Ca^{2+}+SO_4^{2-}) are found to be low with an enrichment in sulfates and a depletion in calcium for most of the samples. This process is elucidated by the basic exchanges with the clay matrix and the precipitation of carbonate minerals. Consequently, two mechanisms of ion exchange coexist, namely direct and reverse exchanges.

Moreover, the phenomenon of dedolomitization is present, caused by the irreversible dissolution of sulfates accompanied by the dissolution of dolomite and calcite precipitation. However, the good correlations between the saturation indices of the waters for halite and gypsum, as a function of (Na^++Cl^-) and (Ca^{2+}+SO_4^{2-}) respectively, support the hypothesis of the dissolution of these evaporites in the waters of both aquifers (CT and CI). Besides, the absence of correlations between the saturation indices of calcite, as a function of (Ca^{2+}+HCO_3^-) and dolomite as a function of (Ca^{2+}+ Mg^{2+}+HCO_3^-), confirms the hypothesis of non-dissolution of these carbonate minerals despite the few cases of undersaturation observed mainly for the CI waters.

Generally, the waters of the aquifer system of the studied area belong to the same geochemical family, with the observation of interference between the two aquifers. This may indicate the presence of an interconnection between these waters, nonetheless this contact is not global but is found in some places. Such discontinuity in the interaction between the studied waters can be directly associated with the fractures or faults affecting the layer separating the two aquifers.

References

Aliev M., (1972). Structures géologiques et perspectives en pétrole et en gaz au Sahara Algérien. [Geological structures and prospects for oil and gas in the Algerian Sahara]. Vol. Tome 1 (Sonatrach). (in French)

ANRH (Agence Nationale des Ressources Hydrauliques) (2005). Inventaire des forages d'eau de la wilaya d'Ouargla. [Inventory of water boreholes in the wilaya of Ouargla]. (Internal report). (in French)

Belkesier M. S., Zeddouri A., Halassa Y., Kechiched R., (20 18). Characterization and geostatistical mapping of water salinity: A case study of terminal complex in the Oued Righ Valley (southern Algeria). 030027. https://doi.org/10.1063/1.5039214

Benmarce K., Hadji R., Zahri F., Khanchoul K., Chouabi A., Zighmi K., Hamed Y. (2021). Hydrochemical and geothermometry characterization for a geothermal system in semiarid dry climate: The case study of Hamma spring (Northeast Algeria). Journal of African Earth Sciences, 182, 104285. https://doi.org/10.1016/j.jafrearsci.2021.104285

Besser H., Redhaounia B., Sana B., Ayadi Y., Khelifi F., Hamed Y. (2019). Geochemical, isotopic and statistical monitoring of groundwater quality: Assessment of the potential environmental impacts of the highly polluted CI water in Southwestern Tunisia. Journal of African Earth Sciences, 153, 144-155. https://doi.org/10.1016/j.jafrearsci.2019.03.001

Bouselsal B., Saibi H. (2022). Evaluation of groundwater quality and hydrochemical characteristics in the shallow aquifer of El-Oued region (Algerian Sahara). Groundwater for Sustainable Development, 17, 100747. https://doi.org/10.1016/j.gsd.2022.100747

Brahmi S., Baali F., Hadji R., Brahmi S., Hamad A., Rahal O., Zerrouki H., Saadali B., and Hamed Y. (2021). Assessment of groundwater and soil pollution by leachate using electrical resistivity and induced polarization imaging survey, case of Tebessa municipal landfill, NE Algeria. Arabian Journal of Geosciences, 14(4), 249. https://doi.org/10.1007/s12517-021-06571-z

BRGM (Bureau de Recherches Géologique et Minière) (1971). Étude hydrochimique de quelques eaux minérales françaises. Applications des méthodes de traitement automatique. [Hydrochemical study of some French mineral waters. Applications of automatic processing methods]. (No. 71-SGN-313-HYD; p. 36). BRGM. http://infoterre.brgm.fr/rapports/71-SGN-313-HYD.pdf (in French)

Cornet A. (1964). Introduction à l'hydrogéologie saharienne. [Introduction to Saharian hydrogeology]. VI : 5-72. (in French)

Dassi L. (2004). Etude hydrogéologique, géochimique et isotopique du système aquifère du bassin de Sbeïtla (Tunisie Centrale). [Hydrogeological, geochemical and isotopic study of the aquifer system of the Sbeïtla basin (Central Tunisia)]. Sfax. (in French)

Dhaouadi L., Besser H., karbout N., Wassar F., Alomrane A. R. (2021). Assessment of natural resources in tunisian Oases: Degradation of irrigation water quality and continued overexploitation of groundwater. Euro-Mediterranean Journal for Environmental Integration, 6(1), 36. https://doi.org/10.1007/s41207-020-00234-3

Drever J. I. (1997). The geochemistry of natural waters: Surface and groundwater environments (3rd ed). Prentice Hall.

Edmunds W. M., Guendouz A. H., Mamou A., Moulla A., Shand P., Zouari K. (2003). Groundwater evolution in the Continental Intercalaire aquifer of southern Algeria and Tunisia: Trace element and isotopic indicators. Applied Geochemistry, 18(6), 805-822. https://doi.org/10.1016/S0883-2927(02)00189-0

Esbensen K. H. (2002). Multivariate Data Analysis: In Practice: An Introduction to Multivariate Data Analysis and Experimental Design (5th ed.).

Fabre J. (1976). Introduction à la géologie du Sahara algérien. [Introduction to the geology of the Algerian Sahara]. SNED. (in French)

Garcia G., del V. Hidalgo M., Blesa M. (2001). Geochemistry of groundwater in the alluvial plain of Tucumán province, Argentina. Hydrogeology Journal, 9(6), 597-610. https://doi.org/10.1007/s10040-001-0166-4

Guendouz A., Moulla A. S., Edmunds W. M., Zouari K., Shand P., Mamou A. (2003). Hydrogeochemical and isotopic evolution of water in the Complexe Terminal aquifer in the Algerian Sahara. Hydrogeology Journal, 11(4), 483-495. https://doi.org/10.1007/s10040-003-0263-7

Hamad A., Abdeslam I., Fehdi Ch., Badreddine S., Mokadem N., Legrioui R., Djebassi T., Rahal O., Hadji R., Hamed Y. (2022). Vulnerability characterization for multi-carbonate aquifer systems in semiarid climate, case of Algerian-Tunisian transboundary basin. International Journal of Energy and Water Resources, 6(1), 67-80. https://doi.org/10.1007/s42108-021-00142-4

Hamed Y., Hadji R., Redhaounia B., Zighmi K., Bâali F., El Gayar A. (2018). Climate impact on surface and groundwater in North Africa: A global synthesis of findings and recommendations. Euro-Mediterranean Journal for Environmental Integration, 3(1), 25. https://doi.org/10.1007/s41207-018-0067-8

Hounslow A. W. (2018). Water Quality Data: Analysis and Interpretation (1st ed.). CRC Press. https://doi.org/10.1201/9780203734117

Kilian C. (1932). Sur les conglomérats précambrien du Sahara Central. Le Pharusien et le Suggarien. [On the Precambrian conglomerates of the Central Sahara. The Pharusian and the Suggarian]. (p. 87). Geological Society of France. (in French)

Kloppmann W., Bourhane A., Asfirane F. (2011). Emploi des outils géochimiques, isotopiques et géophysiques. [Use of geochemical, isotopic and geophysical tools]. (p. 129). (in French)

McLean W., Jankowski J., Lavitt N. (2000). Groundwater quality and sustainability in an alluvial aquifer, Australia.

Moulla A. S., Guendouz A., Cherchali M.E.H. (2002). Contribution des isotopes à l'étude des ressources en eau souterraines transfrontalières en Algérie. [Contribution of isotopes to the study of transboundary groundwater resources in Algeria]. https://doi.org/10.13140/RG.2.1.2253.7369 (in French)

Nadhira S., Omar S. (2019). Hydrogeochemical characterization of the Complexe Terminal aquifer system in hyper-arid zones: The case of Wadi Mya Basin, Algeria. Arabian Journal of Geosciences, 12(24), 793. https://doi.org/10.1007/s12517-019-4917-8

Ncibi K., Hadji R., Hajji S., Besser H., Hajlaoui H., Hamad A., Mokadem N., Ben Saad A., Hamdi M., Hamed Y. (2021). Spatial variation of groundwater vulnerability to nitrate pollution under excessive fertilization using index overlay method in central Tunisia (Sidi Bouzid basin)*. Irrigation and Drainage, 70(5), 1209-1226. https://doi.org/10.1002/ird.2599

Nekkoub A., Baali F., Hadji R., Hamed Y. (2020). The EPIK multi-attribute method for intrinsic vulnerability assessment of karstic aquifer under semi-arid climatic conditions, case of Cheria Plateau, NE Algeria. Arabian Journal of Geosciences, 13(15), 709. https://doi.org/10.1007/s12517-020-05704-0

Nezli I. E. (2009). Approche hydrogéochimique à l'étude des aquifères de la basse vallée de l'Oued M'ya (Ouargla). [Hydrogeochemical approach to the study of aquifers in the lower valley of Oued M'ya (Ouargla)]. Biskra. (in French)

Olivier A. (2005). Chimie et pollutions des eaux souterraines. [Groundwater Chemistry and Pollution]. (in French)

OSS (Observatoire du Sahara et du Sahel) (2003). Système Aquifère du Sahara Septentrional Hydrogéologie. [Northern Sahara Aquifer System Hydrogeology]. (2nd Edition Volume II). Sahara And Sahel Observatory. (in French)

OSS (Observatoire du Sahara et du Sahel) (2015). Pour une meilleure valorisation de l'eau d'irrigation dans le bassin du SASS : Diagnostic et recommandations. [For a better use of irrigation water in the SASS basin: Diagnosis and recommendations]. (p. 35). Sahara And Sahel Observatory. http://www.oss-online.org/index.php/fr/publications/SASS-Recomm-SASS. (in French)

Piper A. M. (1944). A graphic procedure in the geochemical interpretation of water-analyses. Transactions, American Geophysical Union, 25(6), 914. https://doi.org/10.1029/TR025i006p00914

Plummer L. N., Vacher H. L., Mackenzie F. T., Bricker O. P., Land L. S. (1976). Hydrogeochemistry of Bermuda: A case history of ground-water diagenesis of biocalcarenites. Geological Society of America Bulletin, 87(9), 1301. https://doi.org/10.1130/0016-7606(1976)87<1301:HOBACH>2.0.CO;2

Schoeller H. (1962). Les Eaux Souterraines. Hydrologie dynamique et chimique, Recherche, Exploitation et évaluation des Ressources. [Underground Waters. Dynamic and chemical hydrology, Research, Exploitation and evaluation of Resources]. (in French)

SONATRACH (Société Nationale pour la Recherche, la Production, le Transport, la Transformation, et la Commercialisation des Hydrocarbures) (2007). Well Evaluation Conference (p. 536). SONATRACH.

UNESCO (United Nations Educational, Scientific and Cultural Organization) (1972). Etude des ressources en eau du Sahara septentrional. Rapport sur les résultats du projet conclusions et recommandations, Algérie-Tunisie. UNESCO. [Study of the water resources of the northern Sahara. Report on the results of the project conclusions and recommendations, Algeria-Tunisia]. (in French)

Vengosh A. (2003). Salinization and Saline Environments. Treatise on Geochemistry, 9, 333-365. https://doi.org/10.1016/B0-08-043751-6/09051-4